

Duplication of the *MECP2* Region Is a Frequent Cause of Severe Mental Retardation and Progressive Neurological Symptoms in Males

Hilde Van Esch,^{1,*} Marijke Bauters,^{2,*} Jaakko Ignatius,³ Mieke Jansen,² Martine Raynaud,⁴ Karen Hollanders,² Dorien Lugtenberg,⁵ Thierry Bienvenu,⁶ Lars Riff Jensen,⁷ Jozef Géczy,^{8,9} Claude Moraine,⁴ Peter Marynen,² Jean-Pierre Fryns,¹ and Guy Froyen²

¹Centre for Human Genetics, University Hospital Gasthuisberg, and ²Human Genome Laboratory, Centre for Human Genetics, Flanders Interuniversity Institute for Biotechnology, Leuven, Belgium; ³Department of Clinical Genetics, Oulu University Hospital and Oulu University, Oulu, Finland; ⁴Centre Hospitalier Universitaire de Tours, Service de Génétique, Tours, France; ⁵Department of Human Genetics, University Medical Centre, Nijmegen, The Netherlands; ⁶Université Paris-Descartes, Faculté de Médecine, INSERM, Centre National de la Recherche Scientifique, Institut Cochin, Paris; ⁷Max Planck Institute for Molecular Genetics, Berlin; and ⁸Department of Genetic Medicine, Women's and Children's Hospital, and ⁹Department of Paediatrics, University of Adelaide, Adelaide, Australia

Loss-of-function mutations of the *MECP2* gene at Xq28 are associated with Rett syndrome in females and with syndromic and nonsyndromic forms of mental retardation (MR) in males. By array comparative genomic hybridization (array-CGH), we identified a small duplication at Xq28 in a large family with a severe form of MR associated with progressive spasticity. Screening by real-time quantitation of 17 additional patients with MR who have similar phenotypes revealed three more duplications. The duplications in the four patients vary in size from 0.4 to 0.8 Mb and harbor several genes, which, for each duplication, include the MR-related *L1CAM* and *MECP2* genes. The proximal breakpoints are located within a 250-kb region centromeric of *L1CAM*, whereas the distal breakpoints are located in a 300-kb interval telomeric of *MECP2*. The precise size and location of each duplication is different in the four patients. The duplications segregate with the disease in the families, and asymptomatic carrier females show complete skewing of X inactivation. Comparison of the clinical features in these patients and in a previously reported patient enables refinement of the genotype-phenotype correlation and strongly suggests that increased dosage of *MECP2* results in the MR phenotype. Our findings demonstrate that, in humans, not only impaired or abolished gene function but also increased *MECP2* dosage causes a distinct phenotype. Moreover, duplication of the *MECP2* region occurs frequently in male patients with a severe form of MR, which justifies quantitative screening of *MECP2* in this group of patients.

Introduction

Mutations and gross rearrangements of the *MECP2* gene (MIM 300005) are associated with Rett syndrome (MIM 312750), a progressive neurodegenerative disorder that affects almost exclusively females, with an estimated prevalence of ~1 in 10,000–15,000 women. Classical Rett is characterized by progressive loss of intellectual functioning, fine and gross motor skills, and communicative abilities; progressive microcephaly; and the appearance of stereotypic hand movements, after a period of normal development (Hagberg et al. 1983). Additional features, including seizures, ataxia, hyperventilation, scoliosis, and growth retardation are often seen. Mutations and large deletions in the *MECP2* gene

are responsible for up to 80% of the classical Rett cases among girls; the large deletions have made quantitative analysis part of the diagnostic workup in girls with Rett syndrome (Schollen et al. 2003; Ravn et al. 2005). Different genotype-phenotype correlation studies were recently published (Amir et al. 1999; Amir and Zoghbi 2000; Kammoun et al. 2004). Initially, Rett syndrome was considered to be an X-dominant condition lethal in hemizygous males (Zoghbi 1988). However, since the first description of a male patient with an *MECP2* mutation, several additional patients have been identified (Meloni et al. 2000; Orrico et al. 2000). The phenotypes presented by these males cover a large spectrum of neurodevelopmental disorders. The classical Rett syndrome in male patients is seen in those with aneuploidy of the X chromosome and in those who are mosaic for an *MECP2* mutation. Lethal neonatal encephalopathy was reported in males born to asymptomatic or mildly affected carrier mothers who inherited the mutation that normally causes the Rett phenotype in females (Zeev et al. 2002). Milder cases are associated with mutations that do not result in classical Rett in female carriers

Received June 3, 2005; accepted for publication July 5, 2005; electronically published July 29, 2005.

Address for correspondence and reprints: Dr. Hilde Van Esch, Centre for Human Genetics, University Hospital Gasthuisberg, Herestraat 49, B-3000 Leuven, Belgium. E-mail: Hilde.VanEsch@med.kuleuven.ac.be

* These two authors contributed equally to this article.

© 2005 by The American Society of Human Genetics. All rights reserved.
0002-9297/2005/7703-0011\$15.00

Table 1**Primer Sequences Used for qPCR Analysis, with Their Approximate Positions on the X Chromosome**

PRIMER ID	PRIMER SEQUENCE (5'→3')		APPROXIMATE POSITION ON X CHROMOSOME
	Forward	Reverse	
NXF5	gca cac aaa atg tcc acg aaa	acc agg atg gag gtg aag tca	100,900,000
66N11	gag ggt gac ggg aat atc ct	tgg tgg ctg agc gga aa	152,396,750
SLC6A8	gct ggt cag att tgt gct tca g	cca gac ccc aaa ctg cat tc	152,472,000
ABCD1	gaa ggc agc ctt gga aaa ga	ggg caa tag tga agg ctt ctg t	152,522,450
314B3	tgg tgg atg gaa gaa cat tca c	cgg caa ggg ctt cct ctt a	152,618,350
L1CAM	ttc gtt cat tgg cca gta cag t	tgg ccc ctg agc tgt ca	152,649,000
MECP2a	tgc tgg atg aat aac cac aac ac	gaa ggt ctc cag cca tca gaa g	152,826,100
MECP2-5'	tcc cag ctg aga gtc cat ctg	cac gtc ttc tca acc taa tgg aat t	152,924,150
Z49258	gga tgg gac gct gct aca ga	gga cat ggt atc agg tgg act ca	153,058,500
EDMD	cat gca cgc tac cag cag cag tc	gaa tga tgt gcc aga gac cgc	153,131,000
GDI1	cct gca acg aca tca aag aca	ttt gcg ctt cat gtt ctc aa g	153,191,850
G6PD	acg gac gtc atc tga gtt ggt	cac cta ctg cag atg ctg tgt ct	153,325,650
115M6	cca aat gcc gtg cct ctt t	tgg acc acg ttg ggt att ca	153,537,800

(Meloni et al. 2000; Couvert et al. 2001). Although *MECP2* mutations were initially reported as a frequent cause of mental retardation (MR) in males, large cohort studies have shown that these mutations in males are far more rare than initially thought and that careful evaluation of the pathogenicity of each identified missense mutation is required (Bourdon et al. 2003).

Array comparative genomic hybridization (array-CGH) has become the method of choice for the detection of microdeletions and microduplications at high resolution, providing direct information on the genomic position of the aberration. We developed an X-chromosome array with a resolution of 80 kb to screen patients with suspected X-linked mental retardation (XLMR) for X-chromosomal aberrations (Van Esch et al. 2005; Bauters et al., in press). In this way, we identified a small duplication at Xq28, comprising the *L1CAM* (MIM 308840) and *MECP2* genes, in a large family with severe XLMR associated with spasticity. Next, we performed quantitative PCR (qPCR) analysis for the *MECP2* gene in 17 male patients with a comparable phenotype, 2 of whom are from families with indicative linkage to Xq28. In this way, we identified three additional patients with a small duplication at Xq28. Genotype-phenotype correlation studies point to the duplication of *MECP2* as the underlying cause of severe MR, adding a new mechanism for MR-associated mutation of *MECP2* in particular and of XLMR genes in general.

Methods

Consent

The study protocol was approved by the appropriate institutional review board of the University Hospital of

Leuven, Belgium, and informed consent was obtained from the parents of the affected patients and their healthy family members.

Preparation of DNA

Genomic DNA from patients as well as from healthy controls was isolated from peripheral blood by standard procedures. DNA was dissolved in TE buffer at a concentration of 0.33 $\mu\text{g}/\mu\text{l}$ and was stored at 4°C.

Full-Coverage X-Chromosome Array-CGH

Production of the X array, probe preparation, and hybridization on the array were performed essentially as described elsewhere (Van Esch et al. 2005; Bauters et al., in press). These protocols were mainly based on those developed at the Sanger Center (Fiegler et al. 2003). For each hybridization, 3 μg each of the Cy5- and Cy3-labeled probes with a specific activity of 40 was mixed together with 100 μg Cot-1 DNA (Invitrogen) and was hybridized for 40 h at 37°C in humid chambers. Arrays were scanned with the Agilent G2565BA MicroArrayScanner System (Agilent), and the acquired images were analyzed using the ArrayVision software (Imaging Research). Spot intensities were corrected for local background, and only those spots with Cy5 and Cy3 signal intensities at least 1.7-fold above the local background were further analyzed. Data normalization was performed against the mean of the spot ratios of all clones. Clones with opposite aberrant ratios in the color-flip experiments were sequence verified (Bauters et al., in press).

Real-Time Quantitation of DNA Copy Number

We used the comparative ddCt method (Sequence Detection System bulletin 2 [Applied Biosystems]) with SYBR-green for confirmation of our array-CGH data. Primers were designed with PrimerExpress software (Applied Biosystems) and can be found in table 1. We first validated whether the efficiency of amplification of the chosen primer sets was equal to that of the normalizer. A primer set for the *NXF5* locus at Xq22 (Jun et al. 2001) was used for normalization. The validation experiments were performed on fourfold dilutions of genomic DNA, starting with 100 ng in the first dilution. For relative quantitation, the reaction mixtures consisted of qPCR Mastermix Plus for SYBR Green I (Eurogentec), with 500 nM of each primer and 10 ng DNA in a total volume of 25 μ l. After an initial denaturation step for 10 min at 95°C, thermal cycling conditions were 15 s at 95°C and 1 min at 60°C for 40 cycles. Finally, the dissociation curves for each reaction were determined. All samples were run in duplicate on an ABI PRISM 7000 instrument, and two independent runs were performed for all samples.

X Inactivation

Lymphocyte genomic DNA from the female subjects was subjected to the androgen-receptor gene methylation assay for assessment of the methylation status, as described by Allen et al. (1992). A ROX-labeled genotyping marker 100-500 (Applied Biosystems) was added, and the samples were separated on an ABI PRISM 3100 automated DNA sequencer (Applied Biosystems) and were analyzed with GeneScan analysis software (Applied Biosystems) for peak position and area intensity calculations. These data were further processed with the use of Excel.

MECP2 mRNA Expression

Total RNA from 10⁷ Epstein-Barr virus (EBV)-transformed peripheral blood lymphocytes (PBLs) was extracted with 1 ml TRIzol (Invitrogen) in accordance with the manufacturer's instructions. A total of 1 μ g was reverse transcribed with Superscript II (Invitrogen), and genomic DNA was removed by DNaseI (Roche) treatment for 30 min at room temperature. Real-time quantitation by the SYBR-green method was performed on 1/20th of the cDNA with the *MECP2* primers (*MECP2*-cDNA-for: 5'-GCTCCAACAGGATTCCATGGT-3'; *MECP2*-cDNA-rev: 5'-GAGGTCCTGGTCTTCTGAC-TTTTC-3'), as described above. The housekeeping gene β -actin (*bACT*-for: 5'-CACCTGAAGTACCCCATCG-3'; *bACT*-rev: 5'-TGCCAGATTTTCTCCATGTTCG-3') was used for normalization. A validation experiment was performed on serial cDNA dilutions.

Results

Clinical Descriptions of the Patients

Family L36.—This family is of Finnish origin and consists of six affected males in three generations (fig. 1). Affected males are briefly described below, and findings are summarized in table 2.

The index patient, IV.1, the only living affected male, was born after an uneventful pregnancy to healthy parents, with birth parameters in the normal range (weight 4,305 g [90th percentile]; height 53 cm [75th percentile]; occipital-frontal circumference (OFC) 36 cm [90th percentile]). His mother had had a miscarriage 2 years earlier. When he was first examined at age 6 mo, a delay in psychomotor development was noted, with the presence of an increased peripheral muscle tone and axial hypotonia. At 10 mo, posterior asymmetry of the skull was observed, as well as generalized inactivity and hypotonia. Since the patient was 2 years of age, absence seizures had been suspected, but repeated electroencephalogram (EEG) examinations did not reveal any significant pathology. An MRI scan performed at the same age showed no evident structural anomalies but somewhat delayed myelination. Reevaluation at age 14 years showed that the patient had profound MR and did not walk. He had absence of speech and increased and very brisk deep-tendon reflexes in both the upper and the lower limbs. He had prominent ears, flat nasal bridge, and posterior asymmetry of the skull, with a protruding tongue and a tendency to hyperventilate when he was nervous (fig. 1). His vision and hearing were normal, as well as his growth, but he had relative microcephaly (–1 SD). A control MRI was normal. Extensive etiological examinations, including metabolic screening, karyotype, *FMR1* and *MECP2* mutation analysis, and skin and muscle biopsies, were normal.

Individual III.3 was born after an uneventful pregnancy and delivery. Very early, a delay in psychomotor development was noted. He achieved independent sitting and some crawling and was able to walk a few steps with support at age 8 years, but he never stood or walked independently. He did not develop any speech and showed a hypotonic facies, including an open mouth, drooling, and a protruding tongue. His growth was considered normal, but, at age 9 years, his head circumference was 51 cm (10th percentile). He also had occipital asymmetry of the skull and long slender fingers with some clubbing of the nails. Since he was 10 years of age, he had received treatment for epileptic seizures, and EEG showed intermittent spike-wave discharges. He had recurrent respiratory infections and died of pneumonia at age 12 years.

His younger brother, individual III.4, showed a similar

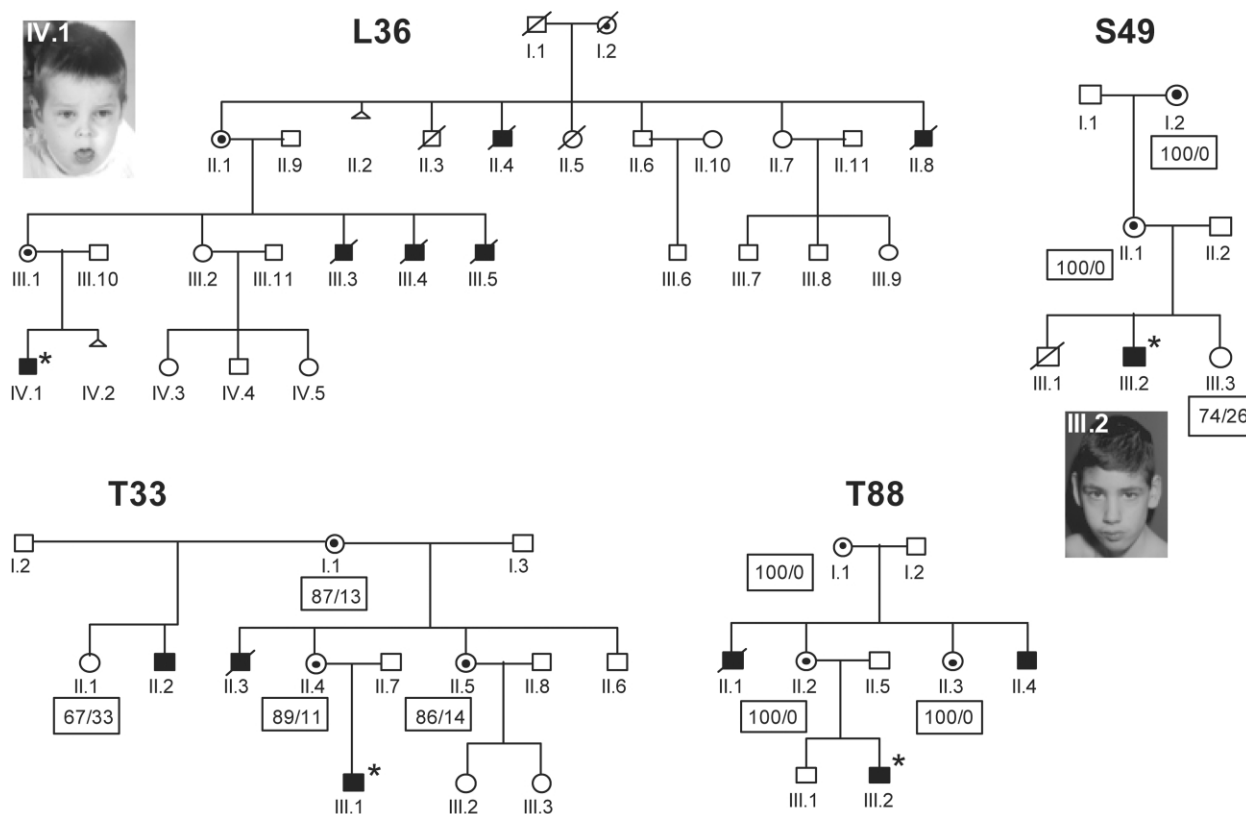


Figure 1 Pedigrees of the four families (L36, S49, T33, and T88) in which duplications at Xq28 have been identified. Blackened squares indicate affected males, and an asterisk (*) indicates the index patient of each family. Clinical pictures of index patients IV.1 (family L36) at age 1.5 years and III.2 (family S49) at age 12 years are shown. Data from X-inactivation studies are boxed and are shown below each female from whom we could obtain a DNA sample.

clinical course. His development was severely delayed, and he was not able to walk or speak. He had frequent and severe respiratory infections, and, at 24 years, he was given the diagnosis of lung tuberculosis. Clinical features similar to the other family members were noted, and his growth was considered relatively normal. He progressively developed spasticity in the lower limbs. At age 24 years, repeated generalized tonic-clonic seizures were noted, with poor response to anti-epileptic treatment. He died at age 35 years of unknown causes.

The third brother, individual III.5, displayed a similar neurological and clinical phenotype, with profound MR and absence of speech. At age 10 years, an inoperable meningioma was diagnosed, and the boy died at age 13 years due to a cerebral herniation caused by the growing tumor. Neuropathology of the brain revealed, in addition to the large meningioma, diffuse gliosis of the white matter, diffuse neuronal loss of the cortex, and some degree of disturbed lamination of the cortex.

The clinical data for individuals II.4 and II.8 are sparse, but, for both, the psychomotor development was

said to be similar to that of individual III.5, with profound MR and absence of speech. They both died in early infancy, probably from pulmonary infections. The cognitive levels of the carrier females and nonaffected males in this family are all within the normal range.

Linkage analysis performed previously on DNA from available living family members, by use of a standard set of polymorphic microsatellite markers spread over the entire X chromosome, assigned the disease locus to the region Xq28-Xqter, with a maximal LOD score of 1.23 at marker *DXS52* at $\theta = 0.0$, with flanking markers *DXS1190* and Xqter. Subsequent mutation analysis of *MECP2*, residing in this genomic interval, did not reveal any mutation in this gene.

Patient S49.—Patient S49 was born to healthy, unrelated parents after a normal pregnancy, with birth parameters within the normal range. He has one younger healthy sister and an older brother with trisomy 21 (fig. 1). In the first years of life, he presented with feeding problems and recurrent upper-airway infections. He was able to walk independently at age 18 mo, but his gait

Table 2**Summary of Clinical Data for the Four Families with an Xq28 Duplication**

CHARACTERISTIC	CLINICAL DATA FOR FAMILY				TOTAL (%)
	L36	S49	T33	T88 ^a	
No. of affected men	6	1	3	3	13
Severe MR	6/6	1/1	3/3	2/2	12/12 (100)
OFC <3rd percentile	1/4	0/1	1/2	0/3	2/10 (20)
Facial hypotonia ^b	4/4	1/1	3/3	3/3	11/11 (100)
Absent speech	6/6	1/1	2/3	1/2	10/12 (83)
Limited speech	0/6	0/1	1/3	1/2	2/12 (17)
Never walked	5/6	0/1	2/3	0/2	7/12 (58)
Limited walking with support	1/6	1/1	1/3	2/2	5/12 (42)
Spasticity (LL > UL)	4/4	1/1	2/2	2/2	9/9 (100)
Seizures	3/4	0/1	0/2	1/2	4/9 (44)
Severe infections	3/6	NA	1/1	1/2	5/9 (56)
Death before age 25 years	4/6	...	1/3	1/2	6/11 (55)

NOTE.—Data are no. of individuals with characteristic/no. of individuals analyzed, unless indicated otherwise. NA = data not available; LL = lower limbs; UL = upper limbs

^a Individual III.2 was only 13 mo of age at evaluation.

^b Facial phenotype for the deceased affected men was scored on the basis of clinical pictures.

was very unsteady and atactic. During childhood, he had two epileptic fits, and he attended a special school. Exhaustive investigations, including evoked potentials and repetitive brain imaging, were all normal. Examination at age 12 years showed an alert boy with normal growth parameters and head circumference but with severe MR and absence of speech (fig. 1). His neurological examination was distinct, with axial hypotonia and spastic diplegia. His behavior was chaotic but social. High-resolution karyotype and *FMR1* analysis were normal.

Family T33.—This family is of French origin, and three males from two generations were affected (fig. 1). The index patient, individual III.1, was first seen at age 4 years by a clinical geneticist. He had been able to walk for a few steps since age 3 years and had developed limited speech. Clinical examination showed a boy with severely delayed development with normal height and weight and a relatively small head circumference (–1 SD). He had bilateral deafness and spasticity in the lower limbs with extension deficit of both knees, together with axial and facial hypotonia. He had a narrow forehead, flat facies, and relatively large, low-set ears. He experienced recurrent respiratory infections. MRI at age 1 year showed no abnormalities except for a cyst of the septum pellucidum and mild cortical atrophy. His mother had two brothers with profound MR, individuals II.2 and II.3. The youngest brother (II.3) died in early infancy at age 3 years. He was profoundly retarded, with absence of speech and motor development. The older half-brother, individual II.2, never learned to speak or walk. Examination at age 24 years showed a man

with profound MR, relatively small stature (156 cm; <3rd percentile), and a head circumference of 55 cm (50th percentile). He progressively developed spasticity, which was more pronounced in the lower limbs, with brisk tendon reflexes and positive Babinski sign. The cognitive levels of the carrier females and nonaffected males in this family are all within the normal range. Exclusion mapping, with a set of 10-cM-spaced X-chromosome markers, that was previously performed on DNA from five available family members excluded the majority of the X chromosome except for the region from Xq27.2 to Xqter.

Family T88.—This family is of French origin and comprises three affected males from two generations (fig. 1). The index patient, individual III.2, was seen at age 13 mo because of developmental delay with pronounced axial and facial hypotonia. His growth parameters were all within the normal range. A CT scan of the brain showed mild enlargement of the ventricles. His mother had two brothers with severe MR. The oldest brother, individual II.1, had profound MR, seizures, absence of speech, and limited motor skills with spasticity, which was more pronounced in the lower limbs. He died at age 24 years due to meningo-encephalitis. The youngest brother, individual II.4, learned to walk at age 2 years and developed limited speech. He has very shy behavior and limited spasticity in the lower limbs. The cognitive levels of the carrier females and nonaffected males in this family are all within the normal range. As with family T33, previously performed exclusion mapping excluded the majority of the X chromosome except the Xq27.2-Xqter region.

Identification and Delineation of a Duplication at Xq28

By X-chromosome array-CGH, we identified a small duplication at Xq28 in family L36. The duplication was evident from aberrant ratios of two adjacent clones (RP11-314B3 and RP11-119A22) at 152.5–152.9 Mb at Xq28 (fig. 2A). The log₂ normalized Cy5/Cy3 ratios obtained for these clones were both 0.7 when the DNA of the L36 index patient was labeled with Cy5 and were both –0.9 when the sample was labeled with Cy3 (array-CGH data are available in online-only appendix A). Analysis of this apparent 0.4-Mb region with the Ensembl and University of California–Santa Cruz (UCSC) genome browsers revealed a gene-dense region including the MR-related *L1CAM* and *MECP2* genes. Other genes within this region are *AVPR2*, *ARHGAP4*, *ARD1*, *RENBP*, *HCFC1*, and *IRAK1*. The X-array clones flanking the duplication, RP11-66N11 (152.3 Mb) and RP5-865E18 (153.3 Mb), showed normal ratios. To delineate the duplication more precisely, real-time quantitation (qPCR) was performed with primer pairs at multiple

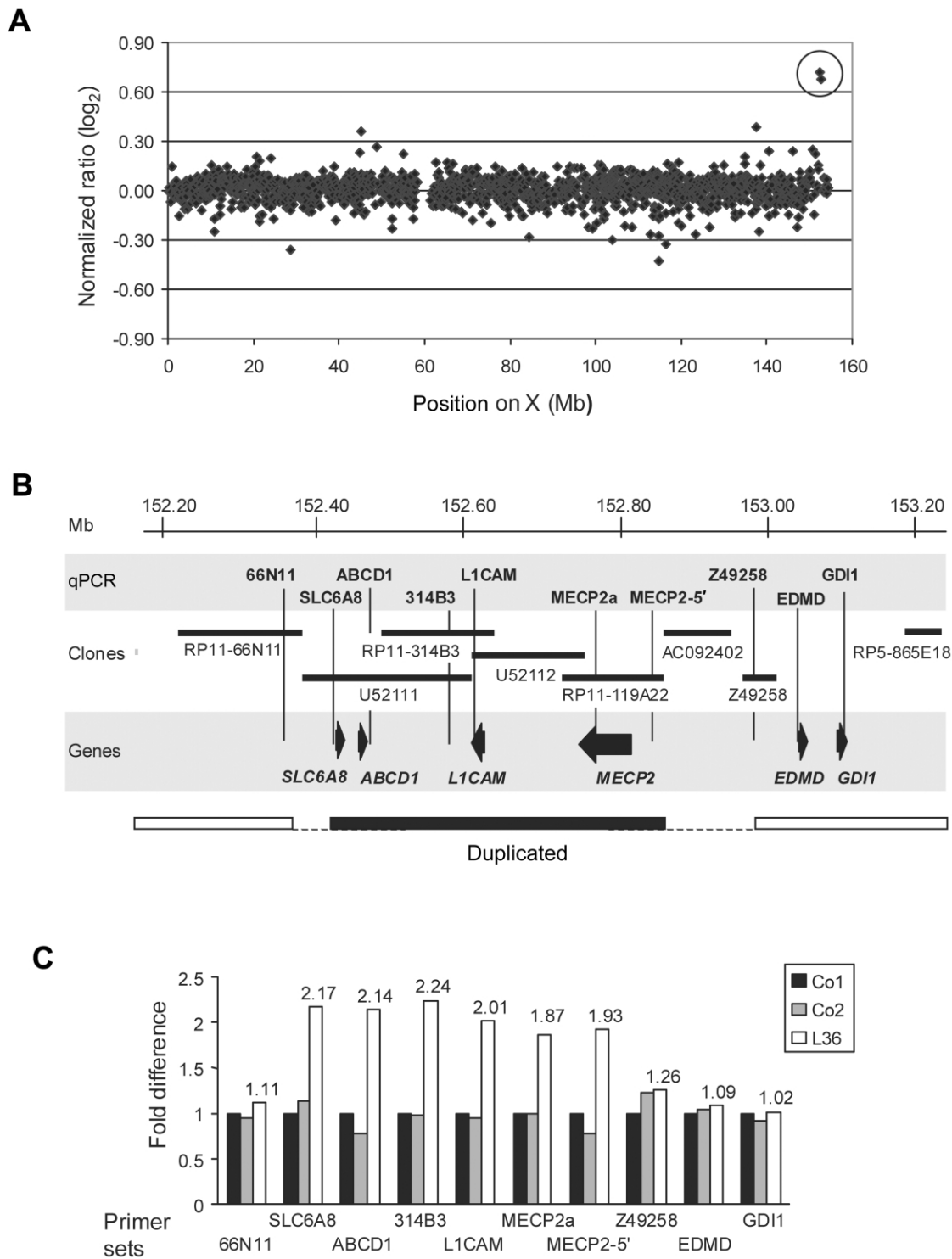


Figure 2 Identification of a duplication at Xq28 in family L36. *A*, X-chromosome array-CGH analysis of DNA (labeled with Cy5) from patient IV.1 mixed with DNA (labeled with Cy3) from a control male. Log₂ normalized ratios are plotted against the position on the X chromosome (in Mb). Except for two polymorphic clones, the ratios for clones in unaffected genomic regions are within the normal interval (−0.36 to 0.36), whereas clones RP11-314B4 and RP11-119A22 at 153 Mb show ratios >0.60 (circled), which is indicative of a duplication. The “gap” at 60 Mb represents the centromeric region for which no clones were available. *B*, Schematic representation of the Xq28 region (152.20–153.20 Mb), showing the location of the qPCR primer sets, genomic clones, and genes present in this interval for which qPCR primers were designed. The duplicated region, based on the array-CGH and qPCR results, is shown below. *C*, qPCR data on DNA from the index patient of family L36 (unblackened bars), as well as from two controls (Co1 and Co2 [blackened bars and gray bars, respectively]). The values for the fold differences obtained for each primer set are given above the bars for the L36 patient only.

positions within and around the identified duplication (fig. 2B). qPCR with primer sets 314B3, L1CAM, and MECP2a, mapping within the aberrant region, confirmed the duplication; the fold differences, relative to control DNA samples, were 2.2, 2.0, and 1.9, respectively (fig. 2C). In addition, the proximally located SLC6A8 and distally located MECP2-5' primer sets revealed fold differences of 2.2 and 1.9, respectively. The values obtained for primer sets at the other tested positions were within the normal interval (1.12 ± 0.1). On the basis of these results, we delineated the duplication within a 580-kb region, with a minimal size of 420 kb (table 1). At the distal breakpoint, the opsin gene repeat cluster (OPN1) is located.

Detection of Three Additional Patients with Small Xq28 Duplications

In the next step, we selected 17 patients with a phenotype similar to that of the index patient of family L36. Of these, 15 were patients with sporadic cases and 2 were index patients from families for which exclusion mapping suggested linkage to the Xq28-Xqter region. For checking of additional duplications, we used the qPCR primer set MECP2a located in intron 2 of the MECP2 gene. Strikingly, we found a duplication at this region in 1 of the 15 sporadic cases and in both of the two patients with familial cases. The fold differences for these three patients were 1.98, 2.47, and 2.54, which are indicative of a copy number of two, whereas this value was 1.02 ± 0.10 for all other samples (fig. 3). Subsequently, the exact position and size of each aberration was checked by qPCR as described above. Figure 4 schematically presents the results of this analysis. The duplication in patient S49, with a minimal and maximal size of 270 kb and 440 kb, respectively, is smaller than that in L36. In T88, the duplication size limits are 540

kb and 660 kb, whereas the largest duplication is found in T33, in which a 0.8-Mb region is involved. The critical region duplicated in all four patients overlaps with that present in S49 and includes the genes from L1CAM to MECP2. The known MR gene SLC6A8 is only involved in family L36, whereas GDI1 is duplicated in family T33. Taken together, the proximal breakpoints of the different duplications are present within a 250-kb region just centromeric of L1CAM. The distal breakpoints are located in a 300-kb interval just telomeric of MECP2 (fig. 4).

Segregation of the Duplication with the Disease

For those family members for whom we could obtain a DNA sample, we analyzed the segregation of the Xq28 duplication by qPCR with the MECP2a primer set. The segregation of the duplication in L36 could only be tested on preserved fibroblast DNA from deceased individual III.4 (fig. 1). He also carried the duplication, since the obtained fold difference by qPCR was 2.16 (fig. 5A). For patient S49, the duplication was also present in his healthy grandmother (I.2) and mother (II.1), who demonstrated fold differences of 1.57 and 1.62, respectively, which is indicative of three copies instead of the normal two (allele ratio in a carrier female vs. a control female is 3/2). His sister (III.3) is not a carrier, since the obtained value was 1.1 (fig. 5A). In families T33 and T88, the aberration was detected in all affected males tested (II.2 and III.1 in T33; II.4 and III.2 in T88) but not in the unaffected males tested (II.6 in T33; III.1 in T88). In the female subjects, all obligate carriers (I.2 and II.1 in S49; I.1 and II.4 in T33; I.1 and II.2 in T88) showed fold differences close to the 1.5 value. Moreover, we were able to identify additional carriers in both families (II.5 in T33; II.3 in T88). Female II.1 in family T33 does not harbor the duplication. X-inactivation studies

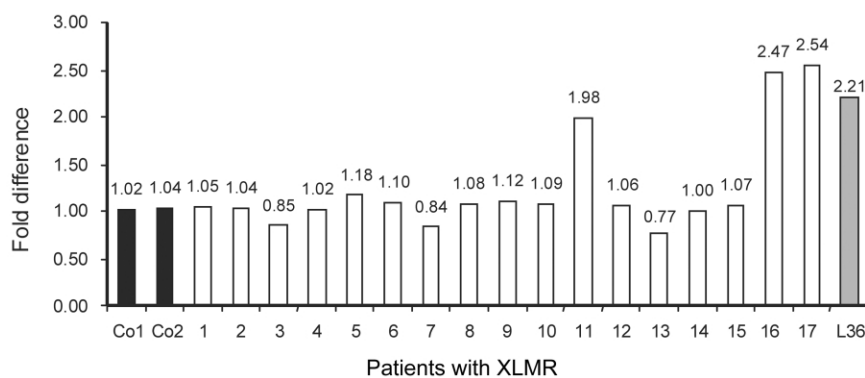


Figure 3 qPCR data obtained by use of the MECP2a primer set for DNA from two controls (Co1 and Co2 [blackened bars]) as well as 17 patients with XLMR (unblackened bars) who showed a phenotype similar to that presented by the index patient of family L36, who was used as a positive control (gray bar). The values for the fold differences in comparison with controls are given above the bars. A duplication was found in three additional patients from families S49 (patient 11), T33 (patient 16), and T88 (patient 17).

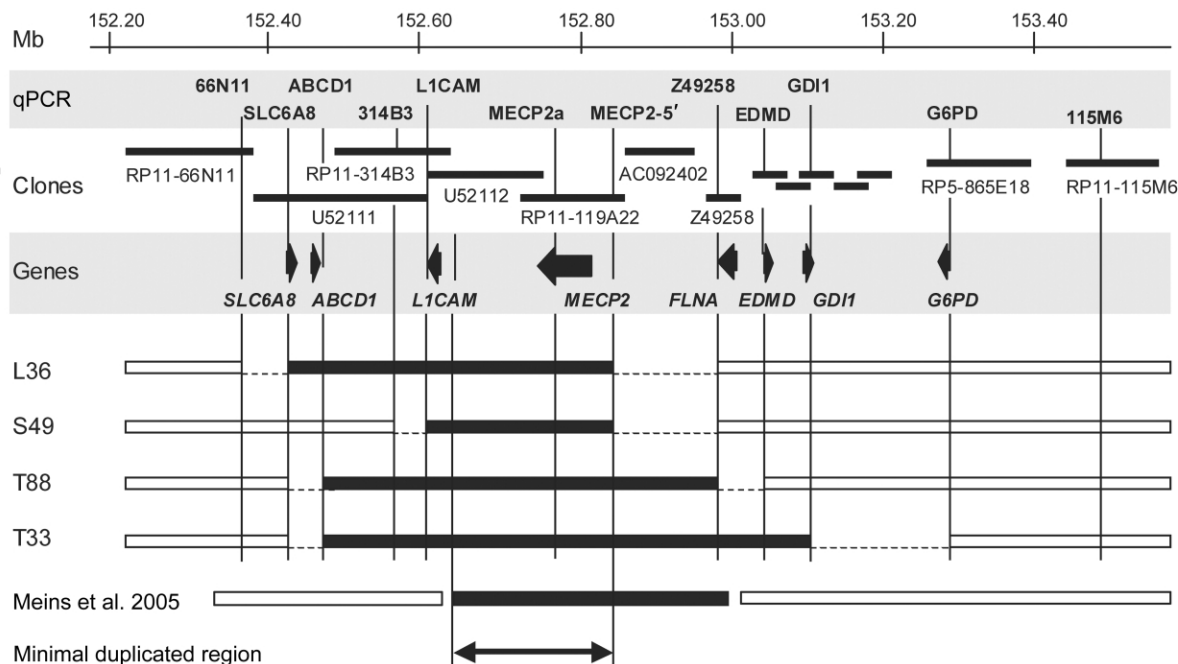


Figure 4 Schematic representation of the positions and sizes of the duplications at Xq28 in the four families with severe MR associated with spasticity. The locations of the qPCR primer sets, genomic clones, and genes present in this interval for which qPCR primers were designed are given. In the lower part, unblackened boxes represent normal regions, and blackened boxes are confirmed duplicated regions. The breakpoints of the duplications are located within the dotted lines. The duplication identified by Meins et al. (2005) is shown at the bottom, as is the common minimal duplicated region in all patients.

showed that all carrier females demonstrated extreme (>85%) or even complete (100%) skewing of one of their X chromosomes (fig. 1). The X-inactivation status in the females with a normal Xq28 dosage, III.3 in S49 and II.1 in T33, were 76/24 and 67/33, respectively. No DNA from female members of the L36 family was available for analysis. *MECP2* mRNA expression was studied by real-time quantitation in EBV-transformed PBL cell lines from the index patients of families L36, T33, and T88. A significantly higher expression was obtained in all cell lines derived from patients carrying the duplication, clearly illustrating a twofold higher expression in these patients than in controls (fig. 5B)

Discussion

X-chromosome-specific array-CGH is a powerful tool to identify submicroscopic aberrations in patients and families with suspected XLMR (Veltman et al. 2004; Van Esch et al. 2005; Bauters et al., in press). By this method, we identified a duplication of ~0.5 Mb at Xq28 in a large family with syndromic MR that encompasses the MR-related *SLC6A8*, *L1CAM*, and *MECP2* genes. The main features present in the affected males in this family were severe-to-profound MR, with onset at birth; axial and facial hypotonia; progressive spasticity, predomi-

nantly of the lower limbs; seizures; and recurrent infections, leading to early death in four of them. The affected males also shared some mild dysmorphic features, including large ears and flat nasal bridge. On the basis of this clinical appearance, we selected a cohort of 17 male patients with a similar phenotype—including patients from two families who have XLMR with suggested linkage to Xq28—for quantitative analysis of the *MECP2* gene. We identified three additional small and overlapping duplications at the Xq28 region, all segregating with the disease in the respective families.

The Xq27-q28 chromosomal region is frequently affected by rearrangements, and at least 16 different males with disomy of the distal part of chromosome Xq have been reported (reviewed by Sanlaville et al. [2005]). In five of them, the disomy is the result of aberrant pairing at the pseudoautosomal Xq-Yq regions (Lahn et al. 1994; Novelli et al. 2004; Teek et al. 2004). In eight patients, the disomies were due to a similar intrachromosomal rearrangement, in which a duplicated Xq26.3-qter or Xq27-qter segment was translocated to the Xp22.3 band (Vasquez et al. 1995; Goodman et al. 1998; Lammer et al. 2001; Kokalj-Vokac et al. 2004). In the remaining three patients, the duplication is the result of a de novo X-autosome translocation (Akiyama et al. 2001; Lachlan et al. 2004; Sanlaville et al. 2005).

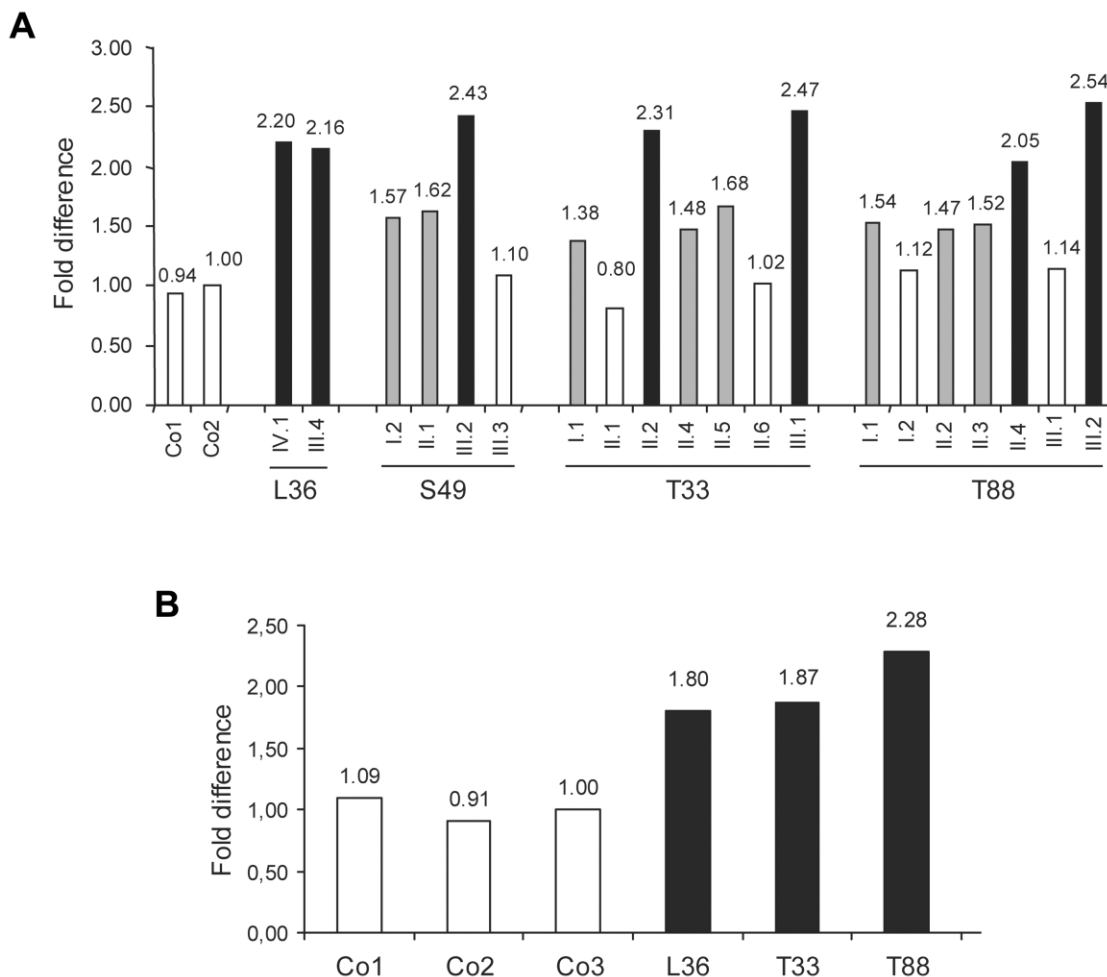


Figure 5 Segregation of the duplication with the disease and increased *MECP2* expression. **A**, Segregation was investigated by qPCR performed using the *MECP2a* primer set on all family members from whom we could obtain a DNA sample. The values for the fold differences in comparison with controls are given above the bars. A blackened bar indicates a male carrier (fold difference ~ 2), and a gray bar indicates a female carrier (fold difference ~ 1.5). **B**, Expression of *MECP2* mRNA, by use of qPCR primers, in PBLs from the index patients of families L36, T33, and T88 (blackened bars), compared with controls (Co1–Co3 [unblackened bars]). The values for the fold differences in comparison with controls are given above the bars.

Compared with our cases, the duplicated regions in these reported patients are much larger, ~ 5 – 12 Mb, and include the pseudoautosomal Xq region. Although the clinical descriptions of these patient are not all complete, they share many clinical features with the patients in this study, including hypotonia, severe MR, mild facial dysmorphism, and proneness to infections (Sanlaville et al. 2005). However, hypoplastic genitalia and cryptorchidism were not observed in our patients. It is of interest that, in our families, the phenotypes are highly similar, even though the duplication sizes are not identical (0.4–0.8 Mb). The common region duplicated in the four families is <450 kb and harbors 10 genes or predicted transcripts (*L1CAM*, *AVPR2*, *ARHGAP4*, *ARD1A*, *RENBP*, *HCFC1*, *Cxorf12*, *IRAK1*, *MECP2*,

and *OPN1MW*), of which only *MECP2* and *L1CAM* are known to be associated with CNS development and function. *L1CAM* codes for the L1 cell-adhesion molecule (CAM) and belongs to a large class of immunoglobulin superfamily CAMs that mediate cell-to-cell adhesion, with highest expression throughout the nervous system (Kenwrick et al. 2000). Mutations in this gene are involved in X-linked hydrocephalus due to stenosis of aqueduct of Sylvius (HSAS [MIM 307000]); MR, aphasia, shuffling gait, and adducted thumbs (MASA [MIM 303350]); and corpus callosum hypoplasia, retardation, adducted thumbs, spastic paraplegia, and hydrocephalus (CRASH [MIM 312900]) syndromes. Thus far, no small duplications that involve only *L1CAM* have been reported, and it is not known if this gene is

associated with a disease phenotype. Overexpression of the L1CAM protein has been reported in different malignant tumors, where it might be involved in the metastasis process (Thies et al. 2002). In the patients of this study who have undergone brain imaging, no brain anomalies were observed that fit with mutated *L1CAM* phenotypes.

Recently, Meins et al. (2005) reported a duplication of ~430 kb within Xq28 in a young boy with severe MR and features of Rett syndrome. The proximal border of this duplication was located 5' of *L1CAM*, leaving this gene intact, whereas the distal border mapped within the *FLNA* gene. Combining their results and ours, we are able to delineate a critical duplicated region, harboring *MECP2* as the only MR-related gene. Therefore, our data suggest that increased gene dosage of *MECP2* is the most likely explanation for the severe MR phenotype present in our patients. We cannot, however, exclude an additional role for *L1CAM* in the neurological phenotype, because the patient of Meins et al. (2005) was not described as having spasticity. On the other hand, the spasticity observed in our families is progressive in nature, and the patient of Meins et al. might have been too young to exhibit this feature. The MR gene *SLC6A8* is duplicated in family L36, whereas, in family T33, *GDI1* is involved in the duplication. Since both are known to play a role in nonspecific MR, a contributive role in the phenotypes of these families cannot be excluded (D'Adamo et al. 1998; Hahn et al. 2002).

Interestingly, several studies have already shown evidence for a dosage-sensitive role for MeCP2 in neuronal plasticity and function. Samaco et al. (2004) performed a high-throughput quantitation of MeCP2 expression on a tissue microarray containing frontal cortex samples from a heterogeneous group of patients with neurodevelopmental disorders and from age-matched controls. By this method, they detected abnormal MeCP2 expression, both decreased and increased, in all samples derived from the patients with a neurodevelopmental disorder, suggesting dysregulation of MeCP2 in these disorders. Elevated *MECP2* mRNA levels, present in our patients, were also detected in lymphoblastoid cells of the patient reported by Meins et al. (2005). Recently, a transgenic mouse model that overexpresses the human *MECP2* gene under the control of its own promoter was reported (Collins et al. 2004). The mice clearly developed a progressive neurological disorder, including seizures and spasticity, and died prematurely. Interestingly, besides the progressive spasticity, the epilepsy subtypes observed in these mice are similar to the absence and tonic-clonic seizures diagnosed in some of the affected men. The neurological phenotype in these animals was modulated by the levels of MeCP2, in that higher protein levels resulted in more-severe pheno-

types. A similar finding was noticed in *Mecp2* knockout mice that were rescued with the mouse *Mecp2* cDNA (Luikenhuis et al. 2004). Increased dosage of the protein to 4–6-fold above normal values resulted in profound motor dysfunction, including side-to-side swaying, tremor, and gait ataxia (Luikenhuis et al. 2004). This dosage sensitivity reflects the necessity of a tight regulation of the *Mecp2* protein level and function in the CNS. Interestingly, Collins et al. (2004) already hypothesized that *MECP2* overexpression could lead to a postnatal neurological phenotype in humans. Additional support for the pathogenicity of the identified X-chromosome aberration is given by the consistent and marked skewing present in the asymptomatic female carriers in these families as well as in the family reported by Meins et al. (2005). Large duplications affecting the Xq28 region have been observed in a number of females, most of whom were phenotypically normal because of the preferential activation of the normal chromosome X, as suggested in the present study in regard to the carrier females. One recent report describes a duplication of the *MECP2* gene in a girl with the preserved-speech Rett variant (Ariani et al. 2004). However, Ariani et al. did not investigate whether the entire gene was duplicated in this female patient.

Altogether, these data point to a tight regulation of MeCP2 expression in pre- and postnatal brain function. This finding puts serious constraints on the applicability of gene therapy for patients with Rett syndrome. Besides the routine quantitative analysis of the *MECP2* gene in female patients who have Rett without a mutation, a diagnostic quantitative workup should also be envisioned for male patients with severe MR and neurological symptoms.

Acknowledgments

We are grateful to the patients and their families, for their cooperation. We thank Mrs. R. Mattlar, Dr. P. Hannikainen, Dr. A. Paetau, and Dr. H. von Koskull, for their help with obtaining blood and tissue samples from family L36, and Dr. C. Goizet, for the information on family T88. H.V.E. is a postdoctoral researcher of the Fund for Scientific Research-Flanders, Belgium (FWO-Vlaanderen). This work was supported by research grant G-0229-01 from FWO-Vlaanderen and by European Union RTD Project QLRT-2001-01810.

Web Resources

The URLs for data presented herein are as follows:

Ensembl Genome Browser, http://www.ensembl.org/Homo_sapiens/

Online Mendelian Inheritance in Man (OMIM), <http://www.ncbi.nlm.nih.gov/Omim/> (for *MECP2* and *L1CAM* and Rett, HSAS, MASA, and CRASH syndromes)

UCSC Human Genome Browser, <http://genome.ucsc.edu/cgi-bin/hgGateway?org=Human>

References

- Akiyama M, Kawame H, Ohashi H, Tohma T, Ohta H, Shishikura A, Miyata I, Usui N, Eto Y (2001) Functional disomy for Xq26.3-qter in a boy with an unbalanced t(X;21)(q26.3;p11.2) translocation. *Am J Med Genet* 99:111–114
- Allen RC, Zoghbi HY, Moseley AB, Rosenblatt HM, Belmont JW (1992) Methylation of *HpaII* and *HhaI* sites near the polymorphic CAG repeat in the human androgen-receptor gene correlates with X chromosome inactivation. *Am J Hum Genet* 51:1229–1239
- Amir RE, Van den Veyver IB, Wan M, Tran CQ, Francke U, Zoghbi HY (1999) Rett syndrome is caused by mutations in X-linked *MECP2*, encoding methyl-CpG-binding protein 2. *Nat Genet* 23:185–188
- Amir RE, Zoghbi HY (2000) Rett syndrome: methyl-CpG-binding protein 2 mutations and phenotype-genotype correlations. *Am J Med Genet* 97:147–152
- Ariani F, Mari F, Pescucci C, Longo I, Bruttini M, Meloni I, Hayek G, Rocchi R, Zappella M, Renieri A (2004) Real-time quantitative PCR as a routine method for screening large rearrangements in Rett syndrome: report of one case of *MECP2* deletion and one case of *MECP2* duplication. *Hum Mutat* 24:172–177
- Bauters M, Van Esch H, Marynen P, Froyen G (2005) X-chromosome array CGH for the identification of novel X-linked mental retardation genes. *Eur J Med Genet* (in press)
- Bourdon V, Philippe C, Martin D, Verloes A, Grandemenge A, Jonveaux P (2003) *MECP2* mutations or polymorphisms in mentally retarded boys: diagnostic implications. *Mol Diagn* 7:3–7
- Collins AL, Levenson JM, Vilaythong AP, Richman R, Armstrong DL, Noebels JL, Sweatt JD, Zoghbi HY (2004) Mild overexpression of *MeCP2* causes a progressive neurological disorder in mice. *Hum Mol Genet* 13:2679–2689
- Couvert P, Bienvenu T, Aquaviva C, Poirier K, Moraine C, Gendrot C, Verloes A, Andres C, Le Fevre AC, Souville I, Steffann J, des Portes V, Ropers HH, Yntema HG, Fryns JP, Briault S, Chelly J, Cherif B (2001) *MECP2* is highly mutated in X-linked mental retardation. *Hum Mol Genet* 10:941–946
- D'Adamo P, Menegon A, Lo Nigro C, Grasso M, Gulisano M, Tamanini F, Bienvenu T, Gedeon AK, Oostra B, Wu SK, Tandon A, Valtorta F, Balch WE, Chelly J, Toniolo D (1998) Mutations in *GDI1* are responsible for X-linked non-specific mental retardation. *Nat Genet* 19:134–139
- Fiegler H, Carr P, Douglas EJ, Burford DC, Hunt S, Scott CE, Smith J, Vetrie D, Gorman P, Tomlinson IP, Carter NP (2003) DNA microarrays for comparative genomic hybridization based on DOP-PCR amplification of BAC and PAC clones. *Genes Chromosomes Cancer* 36:361–374
- Goodman BK, Shaffer LG, Rutberg J, Leppert M, Harum K, Gagos S, Ray JH, Bialer MG, Zhou X, Pletcher BA, Shapira SK, Geraghty MT (1998) Inherited duplication Xq27-qter at Xp22.3 in severely affected males: molecular cytogenetic evaluation and clinical description in three unrelated families. *Am J Med Genet* 80:377–384
- Hagberg B, Aicardi J, Dias K, Ramos O (1983) A progressive syndrome of autism, dementia, ataxia, and loss of purposeful hand use in girls: Rett's syndrome: report of 35 cases. *Ann Neurol* 14:471–479
- Hahn KA, Salomons GS, Tackels-Horne D, Wood TC, Taylor HA, Schroer RJ, Lubs HA, Jakobs C, Olson RL, Holden KR, Stevenson RE, Schwartz CE (2002) X-linked mental retardation with seizures and carrier manifestations is caused by a mutation in the creatine-transporter gene (*SLC6A8*) located in Xq28. *Am J Hum Genet* 70:1349–1356
- Jun L, Frints S, Duhamel H, Herold A, Abad-Rodriguez J, Dotti C, Izaurralde E, Marynen P, Froyen G (2001) *NXF5*, a novel member of the nuclear RNA export factor family, is lost in a male patient with a syndromic form of mental retardation. *Curr Biol* 11:1381–1391
- Kammoun F, de Roux N, Boespflug-Tanguy O, Vallee L, Seng R, Tardieu M, Landrieu P (2004) Screening of *MECP2* coding sequence in patients with phenotypes of decreasing likelihood for Rett syndrome: a cohort of 171 cases. *J Med Genet* 41:e85
- Kenwrick S, Watkins A, De Angelis E (2000) Neural cell recognition molecule L1: relating biological complexity to human disease mutations. *Hum Mol Genet* 9:879–886
- Kokalj-Vokac N, Marcun-Varda N, Zagorac A, Erjavec-Skerget A, Zagradisnik B, Todorovic M, Gregoric A (2004) Subterminal deletion/duplication event in an affected male due to maternal X chromosome pericentric inversion. *Eur J Pediatr* 163:658–663
- Lachlan KL, Collinson MN, Sandford RO, van Zyl B, Jacobs PA, Thomas NS (2004) Functional disomy resulting from duplications of distal Xq in four unrelated patients. *Hum Genet* 115:399–408
- Lahn BT, Ma N, Breg WR, Stratton R, Surti U, Page DC (1994) Xq-Yq interchange resulting in supernormal X-linked gene expression in severely retarded males with 46,XYq- karyotype. *Nat Genet* 8:243–250
- Lammer EJ, Punglia DR, Fuchs AE, Rowe AG, Cotter PD (2001) Inherited duplication of Xq27.2→qter: phenocopy of infantile Prader-Willi syndrome. *Clin Dysmorphol* 10:141–144
- Luikenuis S, Giacometti E, Beard CF, Jaenisch R (2004) Expression of *MeCP2* in postmitotic neurons rescues Rett syndrome in mice. *Proc Natl Acad Sci USA* 101:6033–6038
- Meins M, Lehmann J, Gerresheim F, Herchenbach J, Hagedorn M, Hameister K, Epplen JT (2005) Submicroscopic duplication in Xq28 causes increased expression of the *MECP2* gene in a boy with severe mental retardation and features of Rett syndrome. *J Med Genet* 42:e12
- Meloni I, Bruttini M, Longo I, Mari F, Rizzolio F, D'Adamo P, Devriendt K, Fryns JP, Toniolo D, Renieri A (2000) A mutation in the Rett syndrome gene, *MECP2*, causes X-linked mental retardation and progressive spasticity in males. *Am J Hum Genet* 67:982–985
- Novelli A, Bernardini L, Salpietro DC, Briuglia S, Merlino MV, Mingarelli R, Dallapiccola B (2004) Disomy of distal Xq in males: case report and overview. *Am J Med Genet A* 128:165–169
- Orrico A, Lam C, Galli L, Dotti MT, Hayek G, Tong SF, Poon PM, Zappella M, Federico A, Sorrentino V (2000) *MECP2*

- mutation in male patients with non-specific X-linked mental retardation. *FEBS Lett* 481:285–288
- Ravn K, Nielsen JB, Skjeldal OH, Kerr A, Hulthen M, Schwartz M (2005) Large genomic rearrangements in *MECP2*. *Hum Mutat* 25:324
- Samaco RC, Nagarajan RP, Braunschweig D, LaSalle JM (2004) Multiple pathways regulate *MeCP2* expression in normal brain development and exhibit defects in autism-spectrum disorders. *Hum Mol Genet* 13:629–639
- Sanlaville D, Prieur M, de Blois MC, Genevieve D, Lapierre JM, Ozilou C, Picq M, Gosset P, Morichon-Delvallez N, Munnich A, Cormier-Daire V, Baujat G, Romana S, Veke-mans M, Turleau C (2005) Functional disomy of the Xq28 chromosome region. *Eur J Hum Genet* 13:579–585
- Schollen E, Smeets E, Deflem E, Fryns JP, Matthijs G (2003) Gross rearrangements in the *MECP2* gene in three patients with Rett syndrome: implications for routine diagnosis of Rett syndrome. *Hum Mutat* 22:116–120
- Teek R, Zordania R, Zörjanova T, Tammur P, Bartsch O (2004) Case report: boy with severe hypotonia, hypogenitalism, chronic interstitial pneumonie, and partial X disomy, karyotype 46,X, der(Y)t(X;Y)(q28;q11.2) [poster 0217]. *Eur J Hum Genet* 12:129
- Thies A, Schachner M, Moll I, Berger J, Schulze HJ, Brunner G, Schumacher U (2002) Overexpression of the cell adhesion molecule L1 is associated with metastasis in cutaneous malignant melanoma. *Eur J Cancer* 38:1708–1716
- Van Esch H, Hollanders K, Badisco L, Melotte C, Van Hummelen P, Vermeesch JR, Devriendt K, Fryns JP, Marynen P, Froyen G (2005) Deletion of *VCX-A* due to NAHR plays a major role in the occurrence of mental retardation in patients with X-linked ichthyosis. *Hum Mol Genet* 14:1795–1803
- Vasquez AI, Rivera H, Bobadilla L, Crolla JA (1995) A familial Xp+ chromosome, dup (Xq26.3→qter). *J Med Genet* 32: 891–893
- Veltman JA, Yntema HG, Lugtenberg D, Arts H, Briault S, Huys EH, Osoegawa K, de Jong P, Brunner HG, Geurts van Kessel A, van Bokhoven H, Schoenmakers EF (2004) High resolution profiling of X chromosomal aberrations by array comparative genomic hybridisation. *J Med Genet* 41:425–432
- Zeev BB, Yaron Y, Schanen NC, Wolf H, Brandt N, Ginot N, Shomrat R, Orr-Urtreger A (2002) Rett syndrome: clinical manifestations in males with *MECP2* mutations. *J Child Neurol* 17:20–24
- Zoghbi H (1988) Genetic aspects of Rett syndrome. *J Child Neurol Suppl* 3:S76–S78